A new proposed mechanism of some known drugs targeting the SARS-CoV-2 spike glycoprotein using molecular docking

Tarek Moussa (tarekmoussa@yahoo.com)
Cairo University
Nevien Sabry
National Research Centre

Research Article

Keywords: SARS-Co-2, COVID-19, molecular docking, oseltamivir, hydroxychloroquine

Posted Date: November 13th, 2020

DOI: https://doi.org/10.21203/rs.3.rs-105677/v1

Abstract

COVID-19 is caused by the novel enveloped beta-coronavirus with a genomic RNA closely related to severe acute respiratory syndrome-corona virus (SARS-CoV) and is named coronavirus 2 (SARS-CoV-2). The receptor binding domain (RBD) of the S-protein interacts with the human ACE-2 receptor that enables the initiation of viral entry. Hence, blocking the S-protein interactions by means of synthetic compounds mark the pivotal step for targeting SARS-CoV-2. Most of the six compounds were observed to fit nicely with specific noncovalent interactions, including H bonds, electrostatic, Van der Waals and hydrophobic bonds (pi and sigma bonds). Oseltamivir was found to be the most strongly interacting with the RBD, exhibiting high values of full fitness and low free energy of binding. it formed multiple noncovalent bonds in the region of the active site. Hydroxychloroquine also demonstrated high binding affinity in the solvent accessbility state and fit nicely into the active pocket of the S-protein. The results revealed that these compounds could be potent inhibitors of S-protein that could, to some extent, block its interaction with ACE-2. It is obvious from the 3D structure of SARS-CoV-2 spike protein was changed with the interaction of different drugs, which led to the unsuitability to bind ACE2 receptor. Hence, laboratory studies elucidating the action of these compounds on SARS-CoV-2 are warranted for clinical assessments. Chloroquine, hydroxychloroquine and oseltamivir interacted well with the receptor binding domain of S-protein via noncovalent interactions and recommended as excellent candidates for COVID-19.

Introduction

Coronavirus disease 2019 (COVID-19) occurred sporadically in Wuhan City, China in December 2019, then quickly spread throughout China and the entire world. Severe acute respiratory syndrome-corona virus 2 (SARS-CoV-2) is one the most infectious evolving current pathogen, causing severe respiratory illness and morbidity[1–3]. In the absence of drugs or vaccines, the cornerstone for preventing the spread of infection lies in adopting good personal hygiene, maintaining social distancing, restricting travel and the use of potentially effective natural products and therapeutics[4,5]. Many artificial and natural compounds have been researched to combat SARS-CoV-2. Most target its spike (S) glycoprotein, which facilitates host cell entry, primarily by binding to the host angiotensin-converting enzyme 2 (ACE 2) receptor, present on the surfaces of macrophages, lymphocytes and other immune cells[6–8]. This phenomenon is specific to the receptor binding domain (RBD) of the S-protein that spans from 326-580 amino acids and has unique sites for interaction with ACE-2[9–11].

Chloroquine and hydroxychloroquine, which have been used for malaria prevention and treatment for decades, as well as for the treatment and management of chronic inflammatory diseases such as systemic lupus erythematosus and rheumatoid arthritis, have gained significant focus as possible therapies[12–14]. Lopinavir is an antiretroviral protease inhibitor used in the treatment of HIV-1 infection combined with other antiretrovirals[15]. Oseltamivir is used in the treatment of the flu virus (influenza), ameliorating the symptoms (such as cough, stuffy nose, fever/chills, sore throat, tiredness, aches) and shortens the recovery time within 1-2 days. Darunavir is an antiretroviral medication that is used in treating and preventing HIV/AIDS. It is generally recommended to be used with other antiretrovirals[16,17].

Ibuprofen is a nonsteroidal anti-inflammatory drug (NSAID) class medication that is used to treat pain, fever, and inflammation, which includes painful periods of menstruation, migraines, and rheumatoid arthritis[18].

In this research, we assessed the interaction of Chloroquine, hydroxychloroquine, lopinavir, oseltamivir, darunavir and ibuprofen with the active site of the RBD of the S protein, using Autodock, Swiss dock and Discovery Studio tools.

Methods

Preparation of receptor protein and active site prediction

Based on the literature, the cryo-electron microscopy structure of SARS-CoV-2 S protein (PDB ID: 6VSB) was first analyzed for ligand interacting sites[19,20]. Spike protein is a homotrimer, so we chose chain A for the analysis containing all the respective domains. The active site of the target protein was predicted by using binding site module using Discovery studio[21,22]. The functional active site was present in the receptor binding domain (Leu 335 to Gly 526), which also comprised the specific active site region or loop region (NAG of RCSB: 6VSB, chain A) (Figure 1). The active site residue ASN343 was chosen as the centre of the grid with the following coordinates: spacing: 0.753 Å, XYZ values: 76 126 76, center coordinates: -36.336 23.128 21.195. For site-specific docking, the X-ray diffraction 3D structure of the specific RBD of S protein (PDBID: 6M0J) with resolution 2.32.Å was chosen for interaction with the ligands. The above coordinates were assigned to the 3D structure followed by docking analysis. The 3D structure was energy minimized in solvent medium in Swiss PDB viewer to a free energy level of E= -10990.533 KJ/mol using inbuilt Gromos96 algorithm to obtain the most stable structure of the protein for docking[23,24].

Ligand preparation

The PDB format of the 3D structure of all the ligands were obtained from the drug bank https://www.drugbank.ca/drugs and PubChem https://pubchem.ncbi.nlm.nih.gov/. Chloroquine, hydroxychloroquine, darunavir, lopinavir, oseltamivir, remdesivir and ibuprofen were used as ligands (Figure 2). The ligands were prepared for docking in the Ligand Preparation tool of the Discovery studio. The root was detected for each ligand, which was eventually saved in PDBQT files similar to that of the receptor protein.

Molecular docking and post scoring analysis

The X-ray diffraction structure of the S protein of SARS-CoV-2 (PDBID: 6M0J, 30 Å) was used for the docking analysis (Figure 1). Site specific docking was performed at the active site of the protein prepared using DS studio client 3.5 as described earlier. Then, all the water molecules and heteroatoms were removed in the Autodock tool. Hydrogen atoms were added to the model based on an explicit all atom model. Kollmann charges were added for ensuing interaction with the ligands, and the model was energy minimized. Both the receptor spike protein and the ligands were processed in Autodock tools as described above and converted to PDBQT format. Eight sets of docking poses were exhaustively performed; each set

of Autodock Vina produced 9 conformations; among them, the best pose with RMSD = 0 and lowest free energy of binding was chosen for further analysis. The interacting sites were further visualized in Discovery Studio Visualizer and the 2D interaction and nature and types of bonds were determined. Finally, rescoring of the docked conformations was performed in Swiss dock program with the same attributes for the receptor protein and ligands for better clarity and refinement of ligand protein interactions. The full fitness value was obtained for the best docked site and analyzed with that of Autodock results.

Results

Receptor protein structure and analysis

The 3D conformer of the RBD of S-protein was exposed to forcefield for energy minimization in the solvent state. The energy was found to be -10990.63 Kcal/mol. Secondary structure analysis using PROMOTIF revealed that the RBD mainly comprised beta strands (25.3%) and few alpha helices (11%), in addition to beta turns, helix-turn helix, beta sheets, and gamma strands (63.7%). The active site center represented residue ASN 343 and formed a loop-like structure. Hydrophobicity-hydrophilicity analysis of the RBD residues using Peptide 2.0 software revealed that neutral and hydrophobic amino acids comprised 44.85% an 38.14%, respectively of the total peptides (https://www.peptide2.com/N_peptide_hydrophobicity_hydrophilicity.php), which indicated lower water solubility and more non polar interactions with different compounds. Further analysis using the complete homotrimeric S-protein of SARS-CoV-2 also revealed that the total protein comprised of 42.14% and 41.1% of hydrophobic and neutral amino acids, suggesting that S-protein is mainly hydrophobic and can interact with non-polar compounds (Figure 3).

Docking analysis

The interaction of chloroquine with the RBD was moderately strong (ΔG = -5.5 Kcal/mol) with the specific interacting residues positioned near the active sites (TRP 436, LEU 441). Noncovalent interactions comprised 2 hydrogen bonds, and 5 hydrophobic bonds between the ligand and the receptor residues. The ligand fit into the binding pocket of the receptor with a full fitness of -770.49 (Table 1, Figure 4).

The interaction of hydroxychloroquine was strong (ΔG = -5.8 Kcal/mol) relative to other compounds, with several interacting residues near the active site region, forming 4 hydrogen bonds and 5 hydrophobic interactions. This ligand fit into the central binding pocket of the RBD with a full fitness of -797.05 and conferred maximum stability (Table 2, Figure 5).

Oseltamivir ligand interacted well with the RBD with a binding energy of ΔG = -5.7 Kcal/mol and full fitness of -794.93. Several interacting residues were in the active site (LEU 517, PHE 464 and THR 430) and formed two hydrogen bonds and four hydrophobic bonds (Table 3, Figure 6).

The ligand darunavir interacted less with the RBD with only 1 reside (THR430) forming 2 hydrogen bonds (Table 4, Figure 7) with fitness of -783.37 and binding energy of ΔG = -5.5 Kcal/mol.

The ligand lopinavir did not interact with the RBD residues using either docking approach; only 1 residue (SER 469) formed hydrogen bond near the active site (Table 5, Figure 8) with low fitness of -677.139 and ΔG = -3.6 Kcal/mol.

Ibuprofen also interacted less with the receptor protein. Although it had low binding energy compared to other ligands (ΔG = -6.1 Kcal/mol), the interacting residues were less, and all formed weaker hydrophobic bonds that signified low interaction with the receptor (Table 6, Figure 9).

Discussion

Several medical and molecular trials involving many natural compounds and synthetic compounds used for medication of other diseases and molecular trials are being pursued[25]. Repurposing previously used drugs with health-promoting effects confer several advantages, including reduced costs, faster regulatory approvals and immediate field trials. Until a vaccine is developed, some treatment is imperative to reduce COVID19 mortality and morbidity.

Multiple studies indicate that repurposing chloroquine and hydroxychloroquine can effectively inhibit Coronaviridae infection (including SARS and SARS-CoV-2) *in vitro*[26–29]. Preliminary conflicting clinical evidence from studies in China and France have put the brakes on their ongoing clinical trials[30,31]. Our findings suggested that the interaction of chloroquine and hydroxychloroquine was moderately strong with residues of the RBD of S-protein and fitting well into the binding pocket of the receptor. Therefore, these compounds could also be potent inhibitors of the S-protein function and should be further evaluated in clinical trials. Our study indicates that oseltamivir could be useful for combating COVID-19, in contrast to the study from Wuhan, which observed no positive results[32]. Several clinical trials are testing the efficacy or oseltamivir in treating COVID-19. Oseltamivir is also used in many combinations in clinical trials, such as with chloroquine and flavipiravir[33]. Our findings were agreement with darunavir's antiviral activity *in vitro* against a clinical isolate from a SARS-CoV-2 patient, where darunavir showed no activity against SARS-CoV-2 and the data did not support the darunavir use for COVID-19 treatment[34]. Our finding regarding Lopinavir was in agreement with the study on hospitalized adult patients with severe SARS-CoV-2, where no benefit was observed beyond standard treatment with lopinavir–ritonavir[35]. Similarly, our results for ibuprofen indicated that it may make symptoms worse in COVID-19 patients[38]. They confirmed that the binding of coronaviruses with angiotensin-converting enzyme-2, and the bioavailability of angiotensin-converting enzyme-2 will be increased by the administration of ibuprofen, thus enhancing and potentiating the process of coronavirus infection[36].

Overall, the drugs used in this study such as hydroxychloroquine, chloroquine and oseltamivir conferred highest interactions with the RBD of S-protein of SARS-CoV-2and they are promising as anti-SARS-CoV-2 compounds. Further laboratory studies and field-based clinical trials are warranted to further extrapolate the antiviral outcomes of these compounds.

Conclusions

Hydroxychloroquine, chloroquine and oseltamivir interacted well with the receptor binding domain of S-protein via noncovalent interactions. These compounds are promising candidates for repurposing for the treatment of ongoing coronavirus pandemic. On the other hand, darunavir, lopinavir and ibuprofen were bad candidate for either the prevention or the treatment of COVID-19.

Declarations

Author Contributions: Conceptualization, T.A.A.M. and N.M.S.; methodology, T.A.A.M. and N.M.S.; validation, T.A.A.M. and N.M.S..; formal analysis, T.A.A.M.; investigation, T.A.A.M.; resources, N.M.S.; data curation, T.A.A.M.; writing—original draft preparation, N.M.S.; writing—review and editing, T.A.A.M.; visualization, T.A.A.M. All authors have read and agreed to the published version of the manuscript.

Ethical approval: This article does not contain any studies with human participants or animals performed by any of the authors.

References

1. Zheng J. SARS-CoV-2: an emerging coronavirus that causes a global threat. Int J Biol Sci. Ivyspring International Publisher; 2020;16:1678.
2. Raoult D, Zumla A, Locatelli F, Ippolito G, Kroemer G. Coronavirus infections: Epidemiological, clinical and immunological features and hypotheses. Cell Stress. Shared Science Publishers; 2020;4:66.
3. Rabi FA, Al Zoubi MS, Kasasbeh GA, Salameh DM, Al-Nasser AD. SARS-CoV-2 and coronavirus disease 2019: what we know so far. Pathogens. Multidisciplinary Digital Publishing Institute; 2020;9:231.
4. Chinazzi M, Davis JT, Ajelli M, Gioannini C, Litvinova M, Merler S, et al. The effect of travel restrictions on the spread of the 2019 novel coronavirus (COVID-19) outbreak. Science (80-). American Association for the Advancement of Science; 2020;368:395–400.
5. Madhav N, Oppenheim B, Gallivan M, Mulembakani P, Rubin E, Wolfe N. Pandemics: risks, impacts, and mitigation. Dis Control Priorities Improv Heal Reducing Poverty 3rd Ed. The International Bank for Reconstruction and Development/The World Bank; 2017.
6. Magrone T, Magrone M, Jirillo E. Focus on Receptors for Coronaviruses with Special Reference to Angiotensin-converting Enzyme 2 as a Potential Drug Target-A Perspective. Endocr Metab Immune Disord Drug Targets. 2020;
7. Liu M, Wang T, Zhou Y, Zhao Y, Zhang Y, Li J. Potential role of ACE2 in coronavirus disease 2019 (COVID-19) prevention and management. J Transl Intern Med. Sciendo; 2020;8:9–19.
8. Kruse RL. Therapeutic strategies in an outbreak scenario to treat the novel coronavirus originating in Wuhan, China. F1000Research. Faculty of 1000 Ltd; 2020;9.
9. Wang S, Guo F, Liu K, Wang H, Rao S, Yang P, et al. Endocytosis of the receptor-binding domain of SARS-CoV spike protein together with virus receptor ACE2. Virus Res. Elsevier; 2008;136:8–15.

10. Ortega JT, Serrano ML, Pujol FH, Rangel HR. Role of changes in SARS-CoV-2 spike protein in the interaction with the human ACE2 receptor: An in silico analysis. EXCLI J. Leibniz Research Centre for Working Environment and Human Factors; 2020;19:410.
11. Struck A-W, Axmann M, Pfefferle S, Drosten C, Meyer B. A hexapeptide of the receptor-binding domain of SARS corona virus spike protein blocks viral entry into host cells via the human receptor ACE2. Antiviral Res. Elsevier; 2012;94:288–96.
12. Juurlink DN. Safety considerations with chloroquine, hydroxychloroquine and azithromycin in the management of SARS-CoV-2 infection. CMAJ. Can Med Assoc; 2020;192:E450–3.
13. Rainsford KD, Parke AL, Clifford-Rashotte M, Kean WF. Therapy and pharmacological properties of hydroxychloroquine and chloroquine in treatment of systemic lupus erythematosus, rheumatoid arthritis and related diseases. Inflammopharmacology. Springer; 2015;23:231–69.
14. Picot S, Marty A, Bienvenu A-L, Blumberg LH, Dupouy-Camet J, Carnevale P, et al. Coalition: Advocacy for prospective clinical trials to test the post-exposure potential of hydroxychloroquine against COVID-19. Elsevier; 2020.
15. Sundquist WI, Kräusslich H-G. HIV-1 assembly, budding, and maturation. Cold Spring Harb Perspect Med. Cold Spring Harbor Laboratory Press; 2012;2:a006924.
16. Günthard HF, Saag MS, Benson CA, Del Rio C, Eron JJ, Gallant JE, et al. Antiretroviral drugs for treatment and prevention of HIV infection in adults: 2016 recommendations of the International Antiviral Society–USA panel. Jama. American Medical Association; 2016;316:191–210.
17. Saag MS, Benson CA, Gandhi RT, Hoy JF, Landovitz RJ, Mugavero MJ, et al. Antiretroviral drugs for treatment and prevention of HIV infection in adults: 2018 recommendations of the International Antiviral Society–USA Panel. Jama. American Medical Association; 2018;320:379–96.
18. Bushra R, Aslam N. An overview of clinical pharmacology of Ibuprofen. Oman Med J. Oman Medical Specialty Board; 2010;25:155.
19. Wrapp D, Wang N, Corbett KS, Goldsmith JA, Hsieh C-L, Abiona O, et al. Cryo-EM structure of the 2019-nCoV spike in the prefusion conformation. Science (80-) [Internet]. 2020;367:1260 LP – 1263. Available from: http://science.sciencemag.org/content/367/6483/1260.abstract
20. Ouyang S. Cryo-electron microscopy structure of the SADS-CoV spike glycoprotein provides insights into an evolution of unique coronavirus spike proteins. BioRxiv. Cold Spring Harbor Laboratory; 2020;
21. Sutter J, Li J, J Maynard A, Goupil A, Luu T, Nadassy K. New features that improve the pharmacophore tools from Accelrys. Curr Comput Aided Drug Des. Bentham Science Publishers; 2011;7:173–80.
22. TT Luu T, Malcolm N, Nadassy K. Pharmacophore modeling methods in focused library selection-applications in the context of a new classification scheme. Comb Chem High Throughput Screen. Bentham Science Publishers; 2011;14:488–99.
23. van Gunsteren WF, Billeter SR, Eising AA, Hünenberger PH, Krüger P, Mark AE, et al. Biomolecular simulation: the GROMOS96 manual and user guide. Vdf Hochschulverlag AG an der ETH Zürich, Zürich. 1996;86.

24. Kaplan W, Littlejohn TG. Swiss-PDB viewer (deep view). Brief Bioinform. Henry Stewart Publications; 2001;2:195–7.
25. Wu R, Wang L, Kuo H-CD, Shannar A, Peter R, Chou PJ, et al. An update on current therapeutic drugs treating COVID-19. Curr Pharmacol Reports. Springer; 2020;1.
26. VincentMJ B. Chloro quineisapotentinhibitorofSARScoronavirusinfectionand spread. VirolJ. 2005;2:69.
27. Ferner RE, Aronson JK. Chloroquine and hydroxychloroquine in covid-19. British Medical Journal Publishing Group; 2020.
28. Aljofan M, Gaipov A. Chloroquine and COVID-19: A Light at the End of the Tunnel, or is it Another Train?. Electron J Gen Med. 2020; 17 (4): em207. 2020.
29. Sinha N, Balayla G. Hydroxychloroquine and covid-19. Postgrad Med J. The Fellowship of Postgraduate Medicine; 2020;
30. Vanden Eynde JJ. COVID-19: An Update About the Discovery Clinical Trial. Pharmaceuticals. Multidisciplinary Digital Publishing Institute; 2020;13:98.
31. Chen Z, Hu J, Zhang Z, Jiang S, Han S, Yan D, et al. Efficacy of hydroxychloroquine in patients with COVID-19: results of a randomized clinical trial. MedRxiv. Cold Spring Harbor Laboratory Press; 2020;
32. Wang D, Hu B, Hu C, Zhu F, Liu X, Zhang J, et al. Clinical characteristics of 138 hospitalized patients with 2019 novel coronavirus–infected pneumonia in Wuhan, China. Jama. American Medical Association; 2020;323:1061–9.
33. Rosa SGV, Santos WC. Clinical trials on drug repositioning for COVID-19 treatment. Rev Panam Salud Pública. SciELO Public Health; 2020;44:e40.
34. De Meyer S, Bojkova D, Cinatl J, Van Damme E, Meng CB, Van Loock M, et al. Lack of antiviral activity of darunavir against SARS-CoV-2. Int J Infect Dis. Elsevier; 2020;
35. Cao B, Wang Y, Wen D, Liu W, Wang J, Fan G, et al. A trial of lopinavir–ritonavir in adults hospitalized with severe Covid-19. N Engl J Med. Mass Medical Soc; 2020;
36. Fang L, Karakiulakis G, Roth M. Are patients with hypertension and diabetes mellitus at increased risk for COVID-19 infection? Lancet Respir Med. Elsevier; 2020;8:e21.

Tables

Table 1. Amino acid residues of 6M0J.pdb involved in interaction with **chloroquine (CID: 2719)** for the best docking pose with minimum binding energy

Residues	Donor	Acceptor	Bond type	Bond distance	Binding energy, ΔG (kcal/mol)	Full fitness (Swiss dock)
TRP 436	HE1	N2	Conventional hydrogen bond	3.05	-5.5	-770.49
	C9	-	Hydrophobic bond (Pi-sigma)	3.81		
	-	C15	Hydrophobic bond (Pi alkyl)	4.57		
PHE 374	H30	-	Hydrogen bond (Pi-donor)	3.262		
LEU 368	CL1	-	Hydrophobic bond (alkyl)	4.46		
	-	-	Hydrophobic bond (Pi alkyl)	5.28		
LEU441	C15	-	Hydrophobic bond (alkyl)	4.836		

Table 2. Amino acid residues of 6M0J.pdb involved in interaction with **hydroxychloroquine (CID: 3652)** for the best docking pose with minimum binding energy

Residues	Donor	Acceptor	Bond type	Bond distance	Binding energy, ΔG (kcal/mol)	Full fitness (Swiss dock)
PHE 347	H49	O	Conventional hydrogen bond	3.04	- 5.8	- 797.057
SER 349	HN	O2	Conventional hydrogen bond	2.78		
SER 399	HG	N5	Conventional hydrogen bond	2.44		
ALA 344	-	-	Hydrophobic bond (Pi alkyl)	4.57		
	-	-	Hydrophobic bond (Pi alkyl)	4.63		
ALA 348	CA	N3	Carbon hydrogen bond	3.56		
	-	-	Hydrophobic bond (Pi alkyl)	5.19		
VAL 341	CL1	-	Hydrophobic bond (alkyl)	4.55		
LYS 356	CL1	-	Hydrophobic bond (alkyl)	4.24		

Table 3. Amino acid residues of 6M0J.pdb involved in interaction with **oseltamivir (CID: 65028)** for the best docking pose with minimum binding energy

Residues	Donor	Acceptor	Bond type	Bond distance	Binding energy, ΔG (kcal/mol)	Full fitness (Swiss dock)
THR 430	HG1	O	Conventional hydrogen bond	2.22	- 5.7	- 794.93
LEU 517	HN	O	Conventional hydrogen bond	2.47		
PHE 392	-	C	Hydrophobic bond (Pi alkyl)	4.9		
TYR 396	-	C	Hydrophobic bond (Pi alkyl)	4.82		
PHE 464	C	-	Hydrophobic bond (Pi sigma)	4.99		
	-	-	Hydrophobic bond (Pi alkyl)	3.74		

Table 4. Amino acid residues of 6M0J.pdb involved in interaction with **darunavir (CID: 213039)** for the best docking pose with minimum binding energy

Residues	Donor	Acceptor	Bond type	Bond distance	Binding energy, ΔG (kcal/mol)	Full fitness (Swiss dock)
THR 430	HN	O8	Conventional hydrogen bond	1.99	- 5.5	- 783.237
	O8	OG1	Conventional hydrogen bond	2.91		

Table 5. Amino acid residues of 6M0J.pdb involved in interaction with **lopinavir (DB01601)** for the best docking pose with minimum binding energy

Residues	Donor	Acceptor	Bond type	Bond distance	Binding energy, ΔG (kcal/mol)	Full fitness (Swiss dock)
SER 469	HG	N33	Conventional hydrogen bond	2.59	- 3.6	- 677.139

Table 6. Amino acid residues of 6M0J.pdb involved in interaction with **ibuprofen (CID: 3672)** for the best docking pose with minimum binding energy

Residues	Donor	Acceptor	Bond type	Bond distance	Binding energy, ΔG (kcal/mol)	Full fitness (Swiss dock)
LEU 368	CD1	-	Hydrophopic (Pi-Sigma)	3.43	- 6.1	- 751.343
PHE 342	-	-	Hydrophopic (Pi-pi T shaped)	5.45		
	-	-	Hydrophopic (Pi-alkyl)	5.31		
	-	C8	Hydrophopic (Pi-alkyl)	4.90		
PHE 374	-	-	Hydrophopic (Pi-alkyl)	4.82		
	-	C8	Hydrophopic (Pi-alkyl)	4.83		

Figures

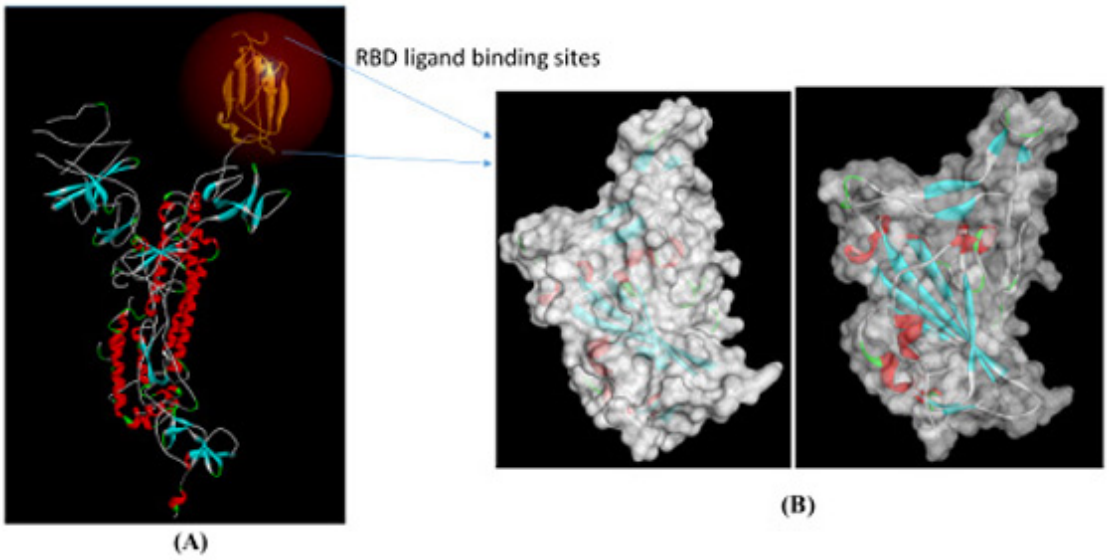

Figure 1

(A) 3D structure cartoon of the monomeric chain of S-protein of SARS-CoV-2 demonstrating the receptor binding region (RBD). (B) The solvent accessibility model of the RBD showing its secondary structure. Alpha helices are in Red. Blue indicates beta sheets. (PDB: 6M0J). The active site region is the loop region selected from the ligand binding sites (NAG of RCSB: 6VSB, chain A) from the above coordinates comprising to Trp 436 to Phe 515. The RBD is the region from Leu 335 to Gly 526.

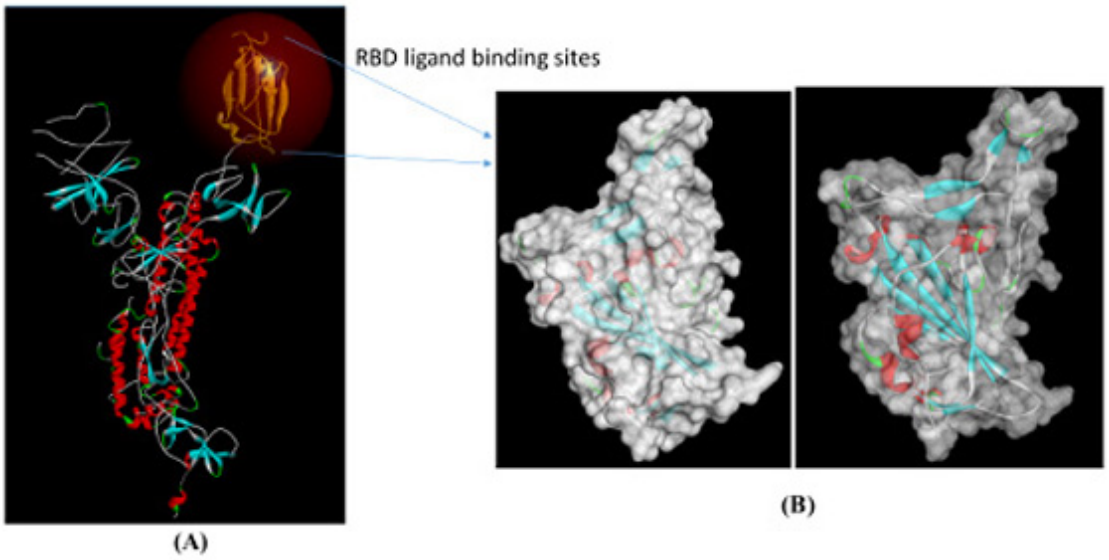

Figure 1

(A) 3D structure cartoon of the monomeric chain of S-protein of SARS-CoV-2 demonstrating the receptor binding region (RBD). (B) The solvent accessibility model of the RBD showing its secondary structure. Alpha helices are in Red. Blue indicates beta sheets. (PDB: 6M0J). The active site region is the loop region selected from the ligand binding sites (NAG of RCSB: 6VSB, chain A) from the above coordinates comprising to Trp 436 to Phe 515. The RBD is the region from Leu 335 to Gly 526.

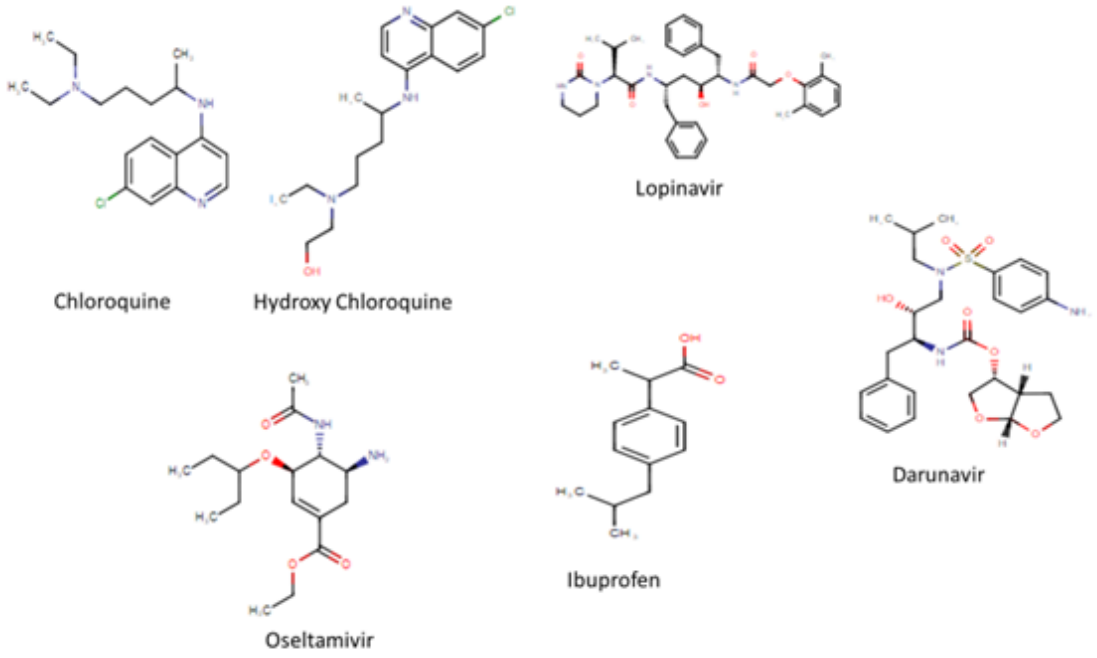

Figure 2

2 D chemical structure of the synthetic compounds used in this study derived from Pubchem and Drug bank.

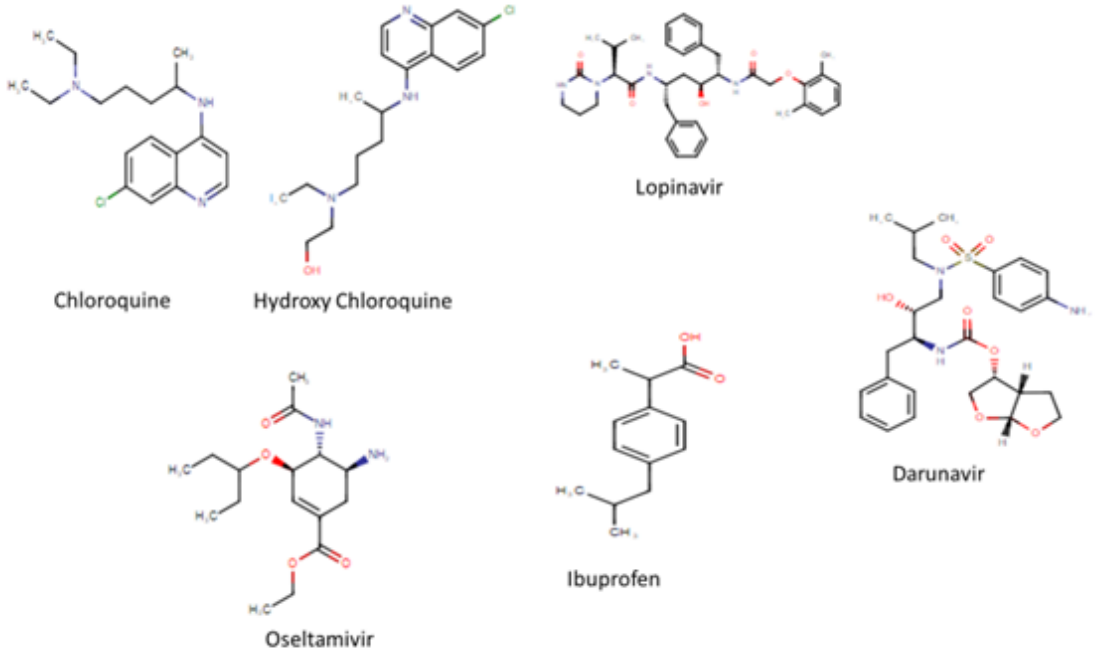

Figure 2

2 D chemical structure of the synthetic compounds used in this study derived from Pubchem and Drug bank.

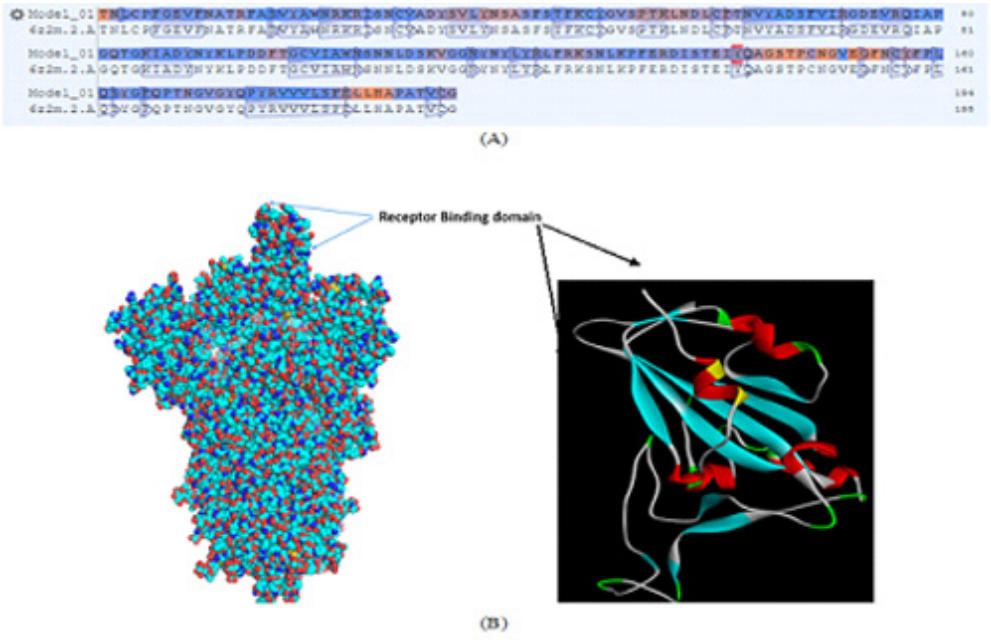

Figure 3

(A) Single sequence alignment of the RBD region (A chain) of 6MoJ amino acid sequence (169 amino acid) with 6yla.2.A; (B) Left: The compact structure of spike glycoprotein showing the receptor binding domain of SARS corona virus 2 (COVID-19), PDB= 6VSB. Right: The structure of specific RBD region of S-protein involved in the ACE2 interaction (PDB= 6M0J).

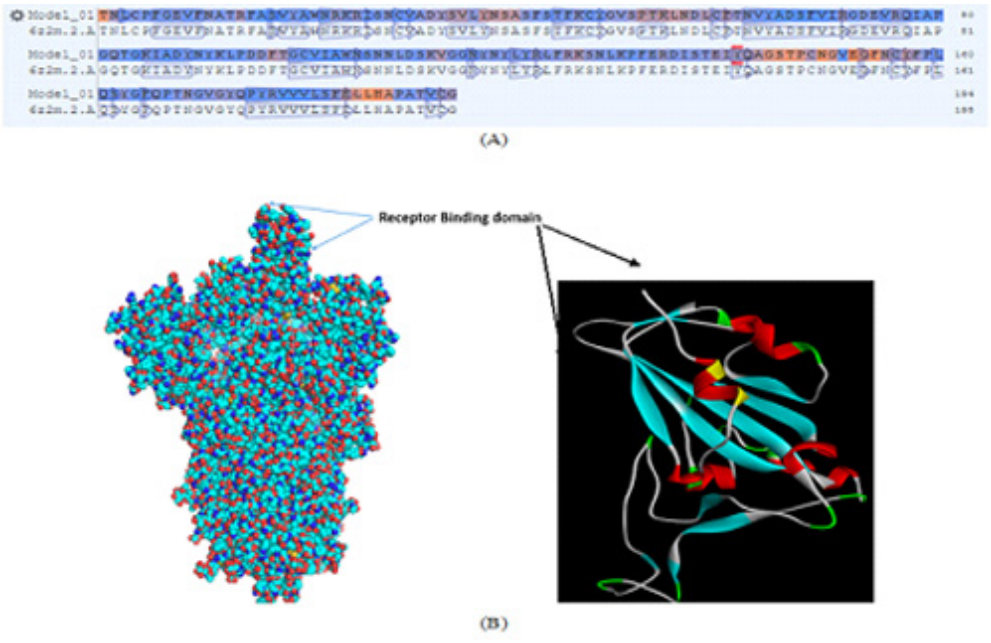

Figure 3

(A) Single sequence alignment of the RBD region (A chain) of 6MoJ amino acid sequence (169 amino acid) with 6yla.2.A; (B) Left: The compact structure of spike glycoprotein showing the receptor binding domain of SARS corona virus 2 (COVID-19), PDB= 6VSB. Right: The structure of specific RBD region of S-protein involved in the ACE2 interaction (PDB= 6M0J).

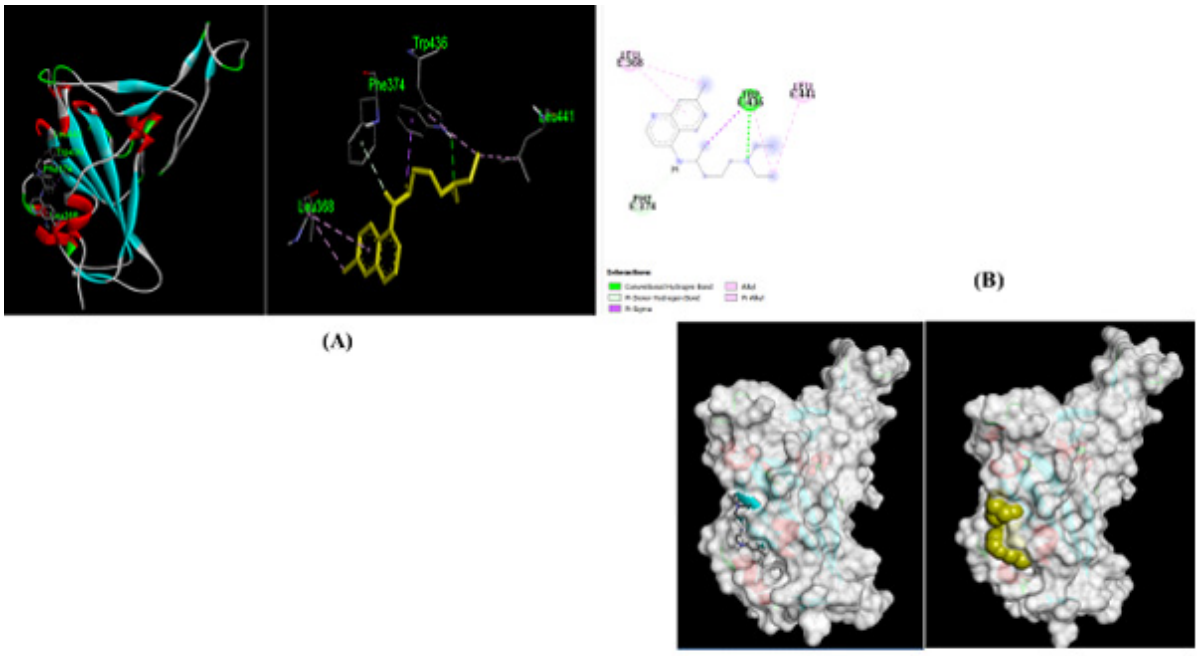

Figure 4

(A) 2D representation of predicted interaction between chloroquine and RBD ligand binding site showing the respective noncovalent interactions. (B) 3D structure model showing the ligand (chloroquine) fitting into the binding pocket of RBD of S-protein. Full fitness: - 770.049, ΔG = -5.5 kcal/mol.

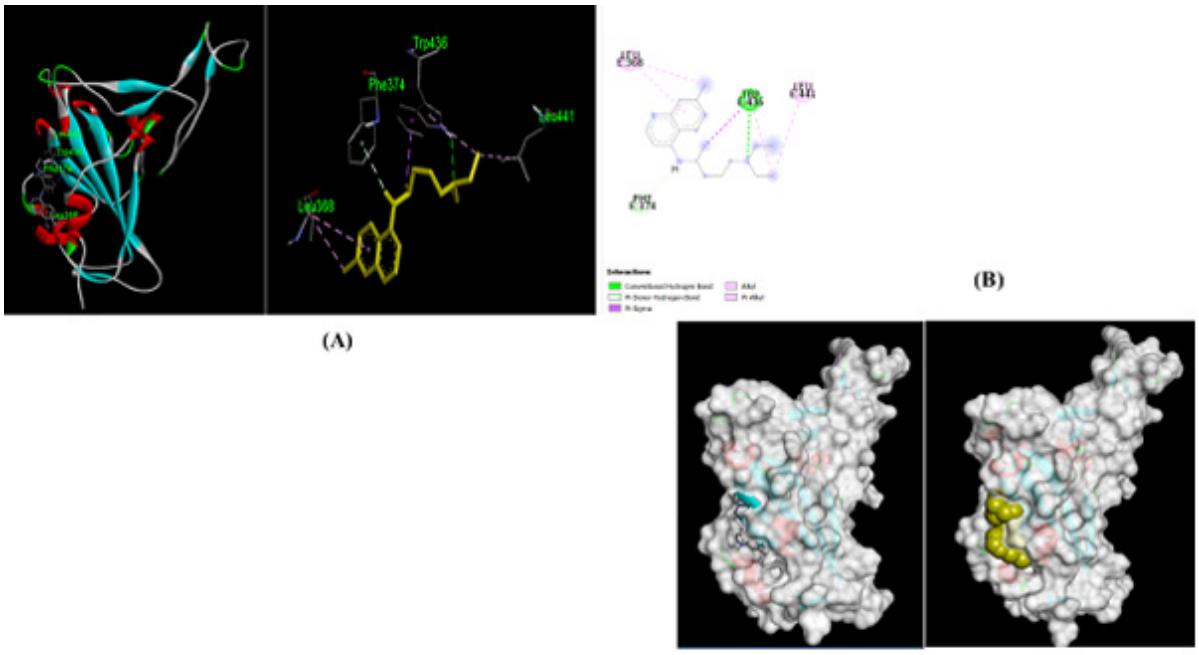

Figure 4

(A) 2D representation of predicted interaction between chloroquine and RBD ligand binding site showing the respective noncovalent interactions. (B) 3D structure model showing the ligand (chloroquine) fitting

into the binding pocket of RBD of S-protein. Full fitness: - 770.049, ΔG = -5.5 kcal/mol.

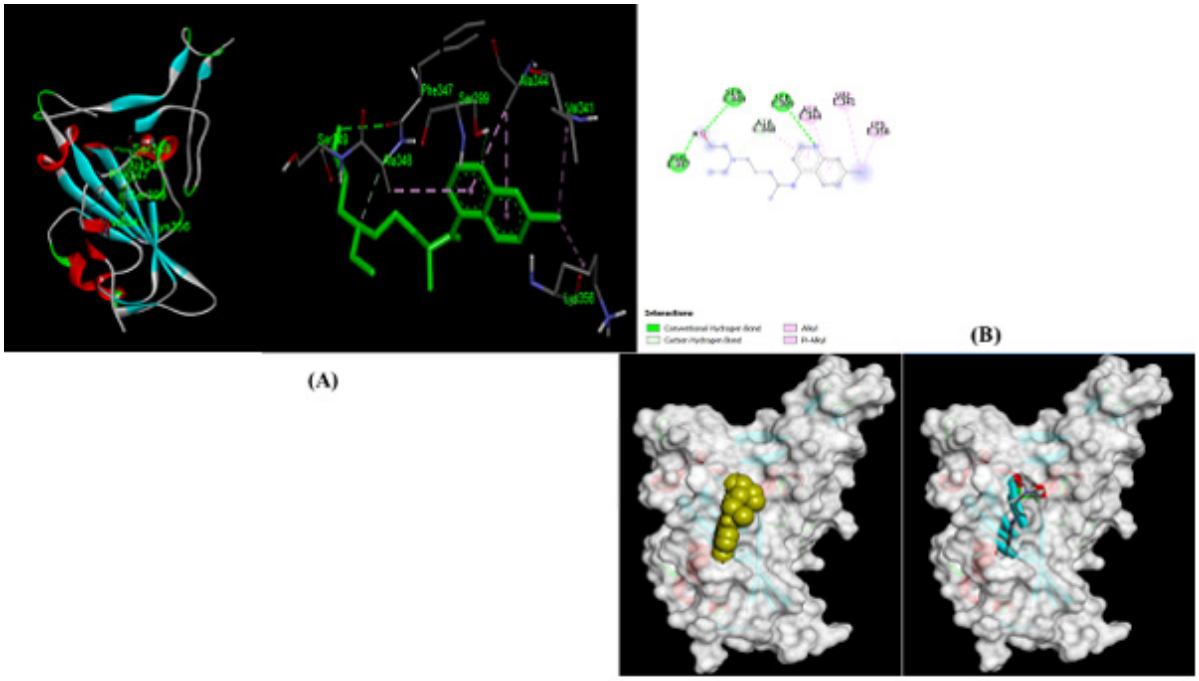

Figure 5

(A) 2D representation of predicted interaction between hydroxychloroquine and RBD ligand binding site showing the respective noncovalent interactions. (B) 3D structure model showing the ligand (hydroxychloroquine) fitting into the binding pocket of RBD of S-protein. Full fitness: - 797.0517, ΔG = 5.8 kcal/mol.

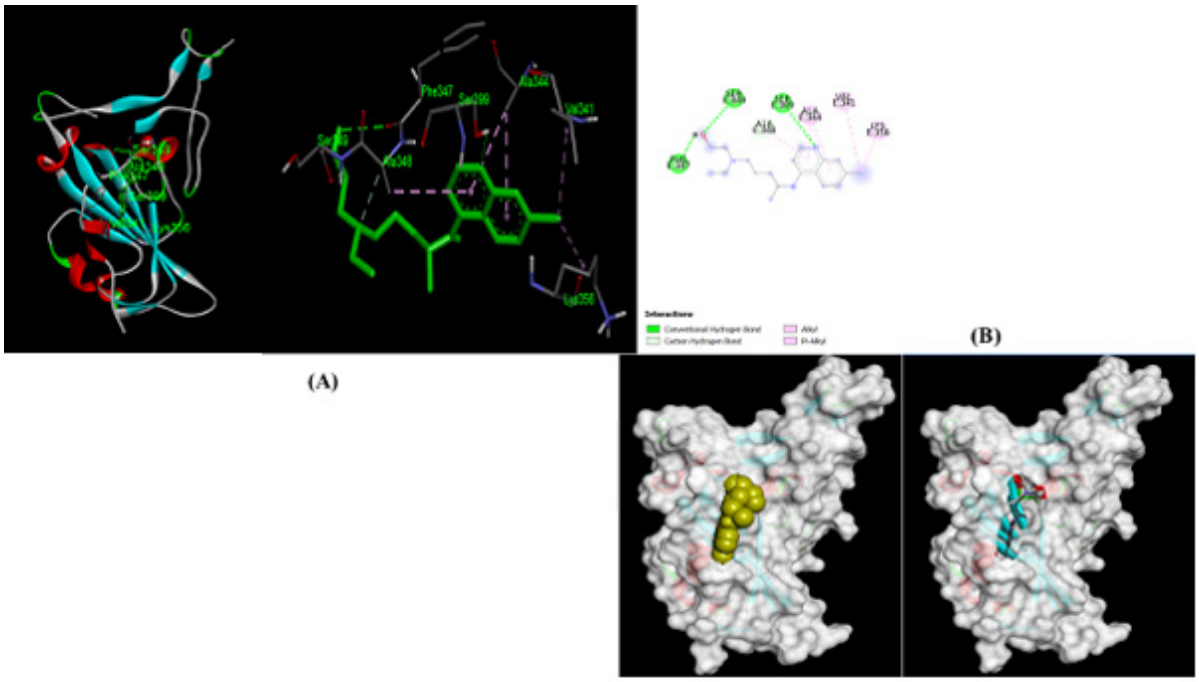

Figure 5

(A) 2D representation of predicted interaction between hydroxychloroquine and RBD ligand binding site showing the respective noncovalent interactions. (B) 3D structure model showing the ligand (hydroxychloroquine) fitting into the binding pocket of RBD of S-protein. Full fitness: - 797.0517, ΔG = 5.8 kcal/mol.

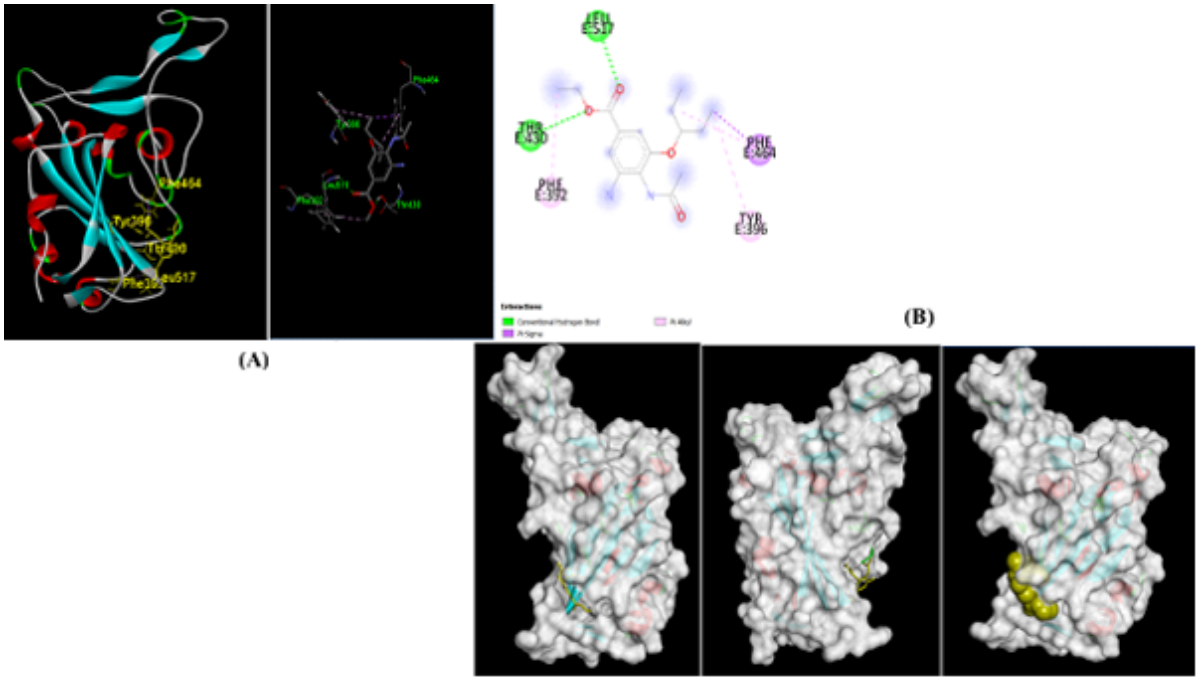

Figure 6

(A) 2D representation of predicted interaction between oseltamivir and RBD ligand binding site showing the respective noncovalent interactions. (B) 3D structure model showing the ligand (oseltamivir) fitting into the binding pocket of RBD of S-protein. Full fitness: - 794.9309, ΔG = -5.7 kcal/mol.

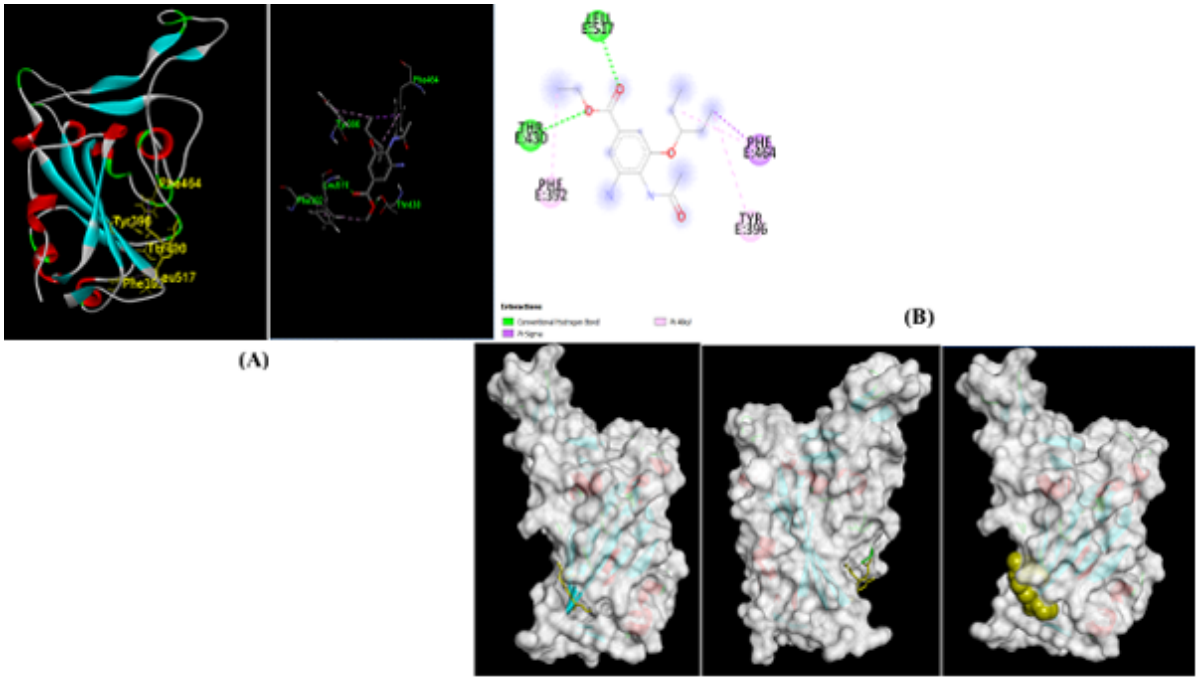

Figure 6

(A) 2D representation of predicted interaction between oseltamivir and RBD ligand binding site showing the respective noncovalent interactions. (B) 3D structure model showing the ligand (oseltamivir) fitting into the binding pocket of RBD of S-protein. Full fitness: - 794.9309, ΔG = -5.7 kcal/mol.

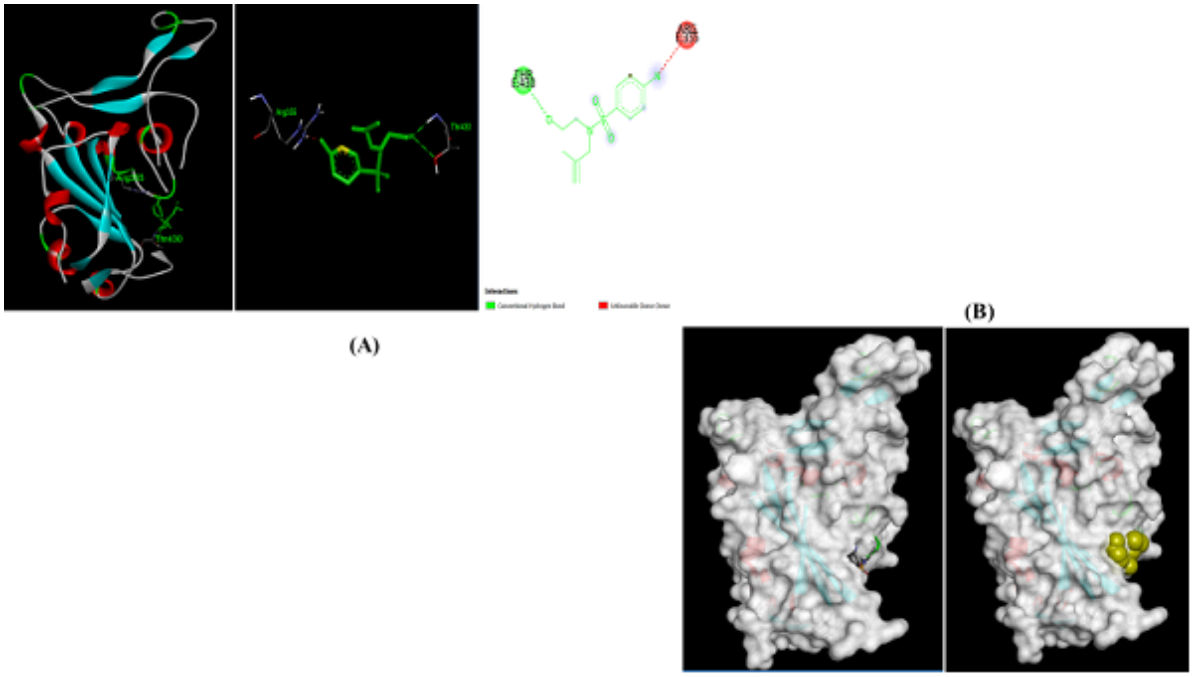

Figure 7

(A) 2D representation of predicted interaction between darunavir and RBD ligand binding site showing the respective noncovalent interactions. (B) 3D structure model showing the ligand (darunavir) fitting into the binding pocket of RBD of S-protein. Full fitness: - 783.237, ΔG= -5.5 kcal/mol.

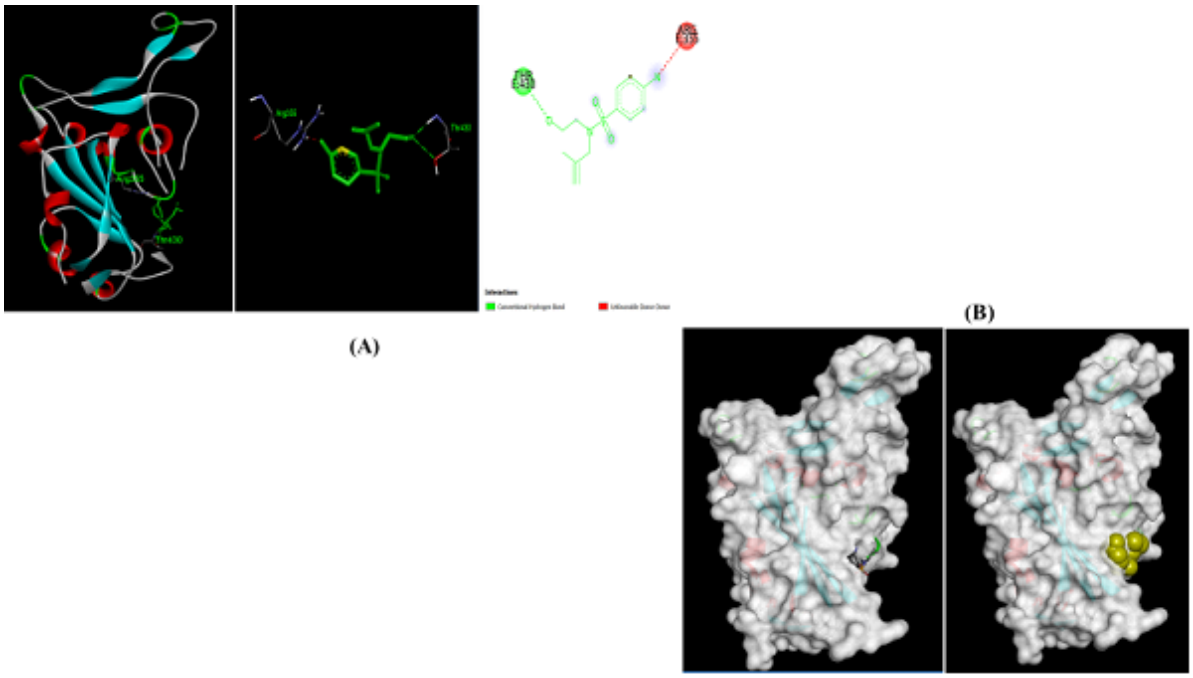

Figure 7

(A) 2D representation of predicted interaction between darunavir and RBD ligand binding site showing the respective noncovalent interactions. (B) 3D structure model showing the ligand (darunavir) fitting into the binding pocket of RBD of S-protein. Full fitness: - 783.237, ΔG= -5.5 kcal/mol.

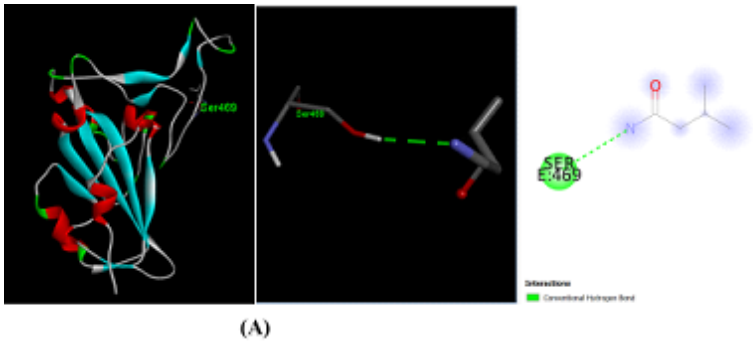

(A)

(B)

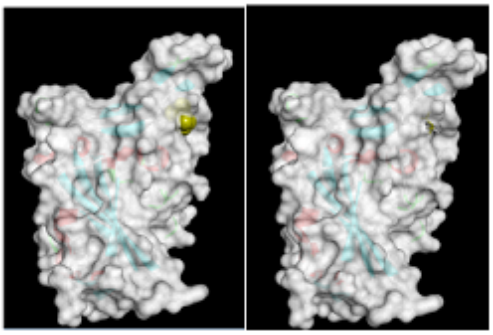

Figure 8

(A) 2D representation of predicted interaction between lopinavir and RBD ligand binding site showing the respective noncovalent interactions. (B) 3D structure model showing the ligand (lopinavir) fitting into the binding pocket of RBD of S-protein. Full fitness: - 677.139, ΔG = -3.6 kcal/mol.

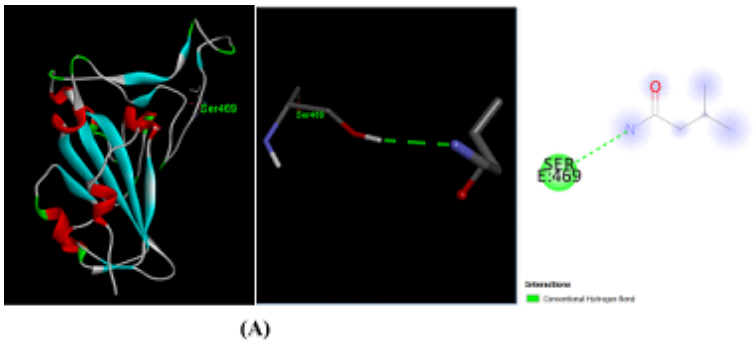

(A)

(B)

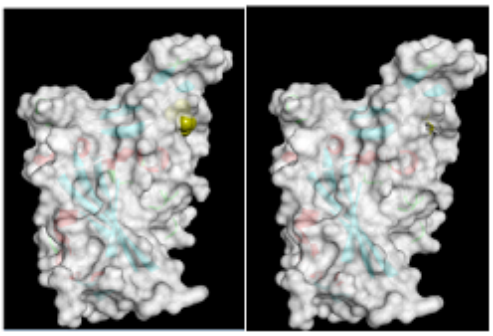

Figure 8

(A) 2D representation of predicted interaction between lopinavir and RBD ligand binding site showing the respective noncovalent interactions. (B) 3D structure model showing the ligand (lopinavir) fitting into the binding pocket of RBD of S-protein. Full fitness: - 677.139, ΔG = -3.6 kcal/mol.

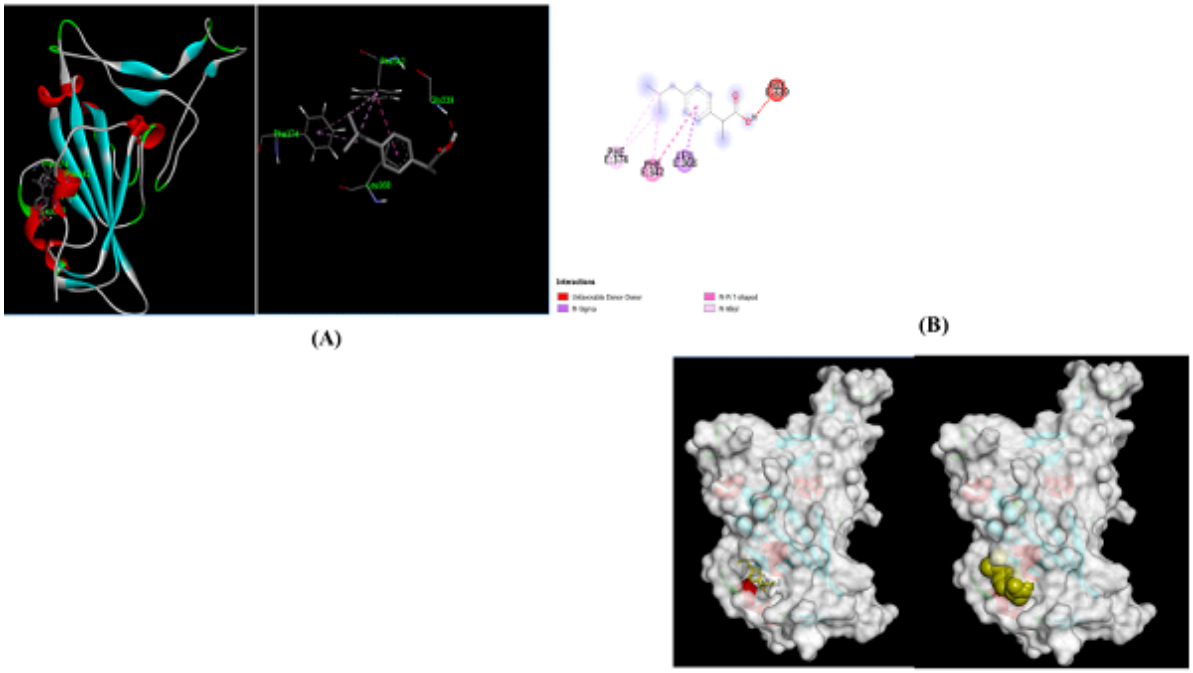

Figure 9

(A) 2D representation of predicted interaction between ibuprofen and RBD ligand binding site showing the respective noncovalent interactions. (B) 3D structure model showing the ligand (Ibuprofen) fitting into the binding pocket of RBD of S-protein. Full fitness: - 751.343, ΔG= -6.1 kcal/mol.

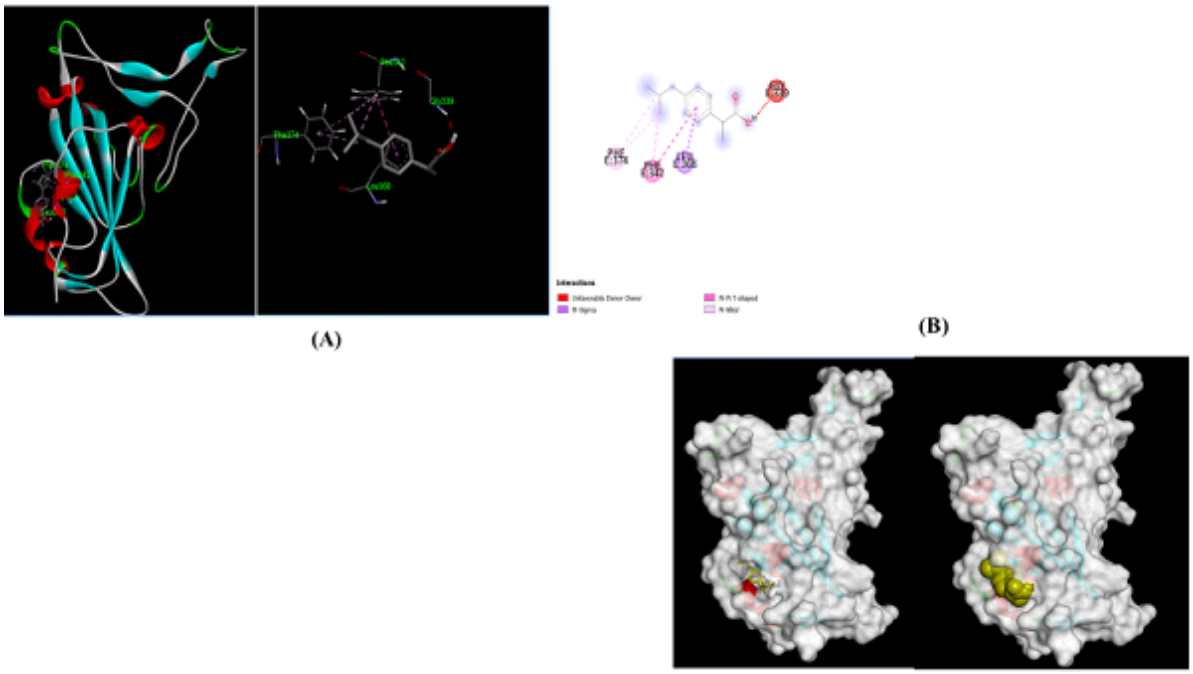

Figure 9

(A) 2D representation of predicted interaction between ibuprofen and RBD ligand binding site showing the respective noncovalent interactions. (B) 3D structure model showing the ligand (Ibuprofen) fitting into the binding pocket of RBD of S-protein. Full fitness: - 751.343, ΔG= -6.1 kcal/mol.